JOURNAL OF MATERIALS SCIENCE 20 (1985) 2623–2629

Hydrogen microprint technique in the study of hydrogen in steels

JOSÉ OVEJERO-GARCÍA
Proyecto Agua Pesada, Comisión Nacional de Energía Atómica, Avenida del Libertador 8250, 1429 Buenos Aires, Argentina

This article considers some fundamental aspects of the hydrogen microprint technique (HMT) recently developed, namely, sensitivity and resolving power, as well as practical considerations like experimental resolving power and spurious corrosion. Finally, applications of HMT to the study of hydrogen distribution in duplex stainless steel, low-carbon steel and austenitic stainless steel have been described. Simplicity and precision are distinct features of this technique, which is proving to be a valuable tool in the study of hydrogen embrittlement of metals and alloys.

1. Introduction

After several years of research, the influence of microstructure on the susceptibility to hydrogen embrittlement of materials has been demonstrated [1, 2]. It is therefore very important to determine the relationship between microstructural elements and hydrogen distribution. Hydrogen bubble analysis [3], neodymium film technique [4] and tritium high-power, high-resolution autoradiography (HPRA) [5] have become standard techniques for revealing the hydrogen distribution on metal surfaces, and also to infer its evolution. HPRA shows on a fine scale the actual distribution of trapped hydrogen (tritium) in microstructural elements such as martensite, microtwins, dislocations [6, 7] and microprecipitates [8].

HMT, described also [9] as silver decoration, was developed recently [10, 11] and is proving to be fairly simple, fast and accurate compared with autoradiography. This work is intended to delve into some fundamental aspects of the technique (sensitivity and resolving power), and also into practical considerations (experimental resolving power and spurious corrosion). Finally, its application to a duplex stainless steel, a low-carbon steel, and an austenitic stainless steel will be described.

2. Experimental procedure

A sample previously charged with hydrogen is covered with a liquid nuclear emulsion containing AgBr crystals (Fig. 1). Hydrogen evolving from the metal surface reduces silver ions to metallic silver. After the desired exposure time, the sample is placed in a fixer which washes away the unreacted AgBr crystals. After rinsing with water and drying, the silver grains are visible in the scanning electron microscope (SEM) as white, spherical particles superimposed on the microstructure. Fig. 2 shows a diagram of the procedure. It is believed helpful to include a few pratical hints for the benefit of would-be users of this technique.

2.1. Metallographic preparation and hydrogen charge

The specimen surface is polished with 0.25 μm diamond paste, and a cathodic hydrogen-charge is introduced at room temperature. The charging conditions depend on the material and on the intended study.

After charging, a slight polishing with 0.25 μm diamond paste is often helpful to eliminate hydrogen adsorbed on the surface. Finally, the microstructure is revealed by etching. In studies of hydrogen diffusivity, cathodic charge is

0022–2461/85 $03.00 + .12

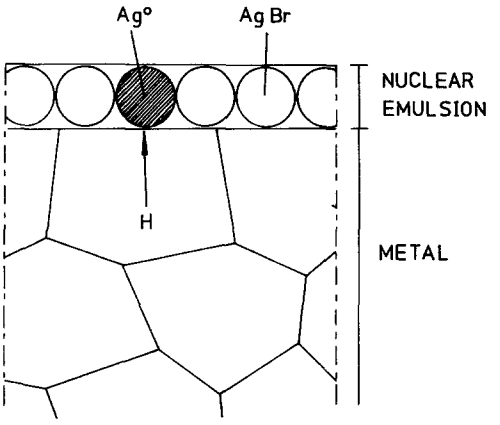

Figure 1 Principle of hydrogen microprint technique.

introduced on the face opposite to the polished one and the last polishing is then unnecessary.

2.2. Nuclear emulsion coating

A thorough study on HPRA at the Physical Metallurgy Laboratory, Orsay (France) [8, 12, 13] provided the basis for preparation of the nuclear emulsion and coating of samples. Ilford L-4 emulsion with a grain size close to 140 nm and a base of gelatin were adopted.

As in the case of HPRA, the success of HMT hinges on obtaining a truly monogranular, densely packed layer of AgBr crystals [13]. This condition is achieved by diluting 1 g emulsion into 2 ml distilled water [12]. The AgBr emulsion sometimes causes a spurious corrosion on the surface under study. It was found [14] that substituting 2 ml of a 5 wt % solution of $NaNO_2$ for the 2 ml of distilled water diminishes this undesirable effect. After dilution, the emulsion is liquified in a water bath at 45° C and held for about 20 min between 45 and 50° C to allow for homogenization, before cooling to room temperature.

A monogranular AgBr emulsion layer is obtained by means of a loop about 5 cm in diameter of thin metal wire (e.g. 0.2 mm diameter) [12]. It is laid on the specimen surface, on which it hardens quickly to gel consistency, hindering the redistribution of AgBr crystals.

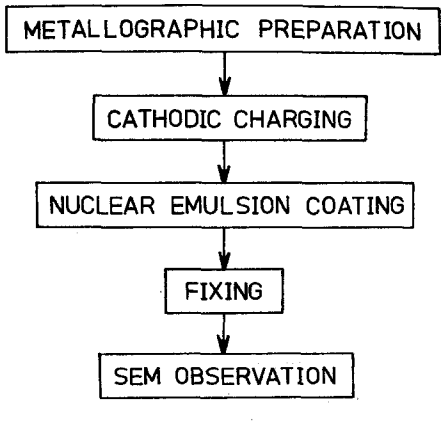

Figure 2 Experimental procedure.

2.3. Fixing

Hydrogen flux from the metal acts on the emulsion for the desired time (typically one hour) causing the reduction of silver ions. An important feature of our technique is that fixing is done under normal illumination. In fact, no darkroom is required as is the case with HPRA, where tritium β rays induce a latent image which must be protected from light photons until fixing removes the unexcited AgBr crystals. The fixing solution is as follows:

Sodium hyposulphite	250 g
Sodium sulphite	10 g
Sodium bisulphate ($\delta = 1.32\,g\,cm^{-3}$)	$50\,cm^3$
Distilled water	to make 1 litre

As in the case of the emulsion, $NaNO_2$ can be added to the fixer to avoid corrosion, at the rate of 30 g of nitrite to each litre of fixer.

After fixing approximately for 3 min, the emulsion-coated sample is rinsed thrice with distilled water; the first and second rinses take about 30 sec and the last 3 min. After drying, the sample is ready for observation with the SEM (Philips PSEM 500).

3. Characteristics of HMT

3.1. Sensitivity

This can be defined as the minimum difference which is observed between hydrogen fluxes from different sources in the same sample. With this definition, sensitivity depends on emulsion efficiency, that is on the ratio of the number of silver grains seen by SEM to the number of hydrogen atoms crossing a given area of emulsion.

Emulsion efficiency is linked to its manufacturing process. Besides this variable, which is beyond the experimenter's control, it is known that the application of nuclear emulsions in monogranular, compact layers leaves 15 to 20% of the surface uncovered by AgBr crystals, due

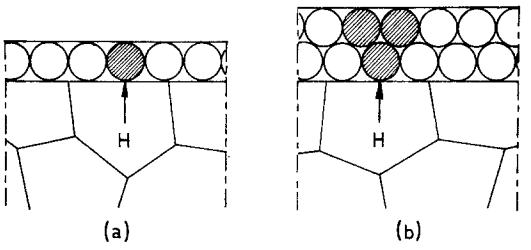

Figure 3 Relationship between emulsion thickness and power of resolution (PR) for (a) an AgBr monolayer, and (b) two AgBr layers.

to interstices between spherical crystals [13]. Some hydrogen atoms are bound to cross through these interstices without interacting with AgBr crystals and, finally, it is difficult to get a theoretical estimate of sensitivity. However, it is possible to find the appropriate experimental conditions for each emulsion, so that a correlation can be established between hydrogen flux and the number of observed silver grains.

3.2. Power of resolution

Silver grains (image) derived from the reaction

$$Ag^+ + H^0 \rightarrow Ag^0 + H^+$$

can be coincident with the hydrogen-source from which they derived, or else located at a certain distance from it. This distance is called the power of resolution (PR) of the technique. Another suitable definition of the PR could be the minimum distance between two hydrogen sources giving distinct images.

The PR depends mainly on the crystal size and the thickness of emulsion coating, being inversely related to both factors (Fig. 3). Under appropriate experimental conditions, i.e. when hydrogen flux is provided mostly by surface sources (cracks, grain boundaries, slip lines) and not by general lattice effusion, one can estimate the PR after Moulin [15].

As shown in Fig. 4, a point source of hydrogen is located in the most unfavourable case, i.e. facing an interstice. Spherical AgBr crystals are assumed to be close packed. The PR in this case is 40 nm.

The gelatin base has an important influence on PR. As already mentioned, it precludes the redistribution of AgBr crystals after gelation while the coating is under hydrogen flux.

The above estimate of PR is compared now with experimental data. HMT was applied to austenitic stainless steel under average conditions, i.e. monogranular layer and medium hydrogen evolution [11]. A given set of slip lines within metal grains were selected as sources of the hydrogen, which had been introduced cathodically. Following Moulin [15], all the silver grains associated with the set were considered and their distance from the host line measured. Under SEM observation there is a variety of sizes of silver grain. The percentage of cumulative frequencies of the measured distances was

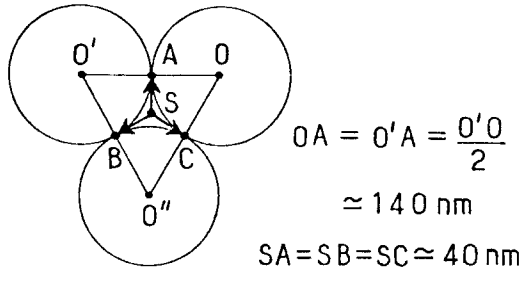

Figure 4 Layout for the calculation of a theoretical PR; point source of hydrogen located between AgBr grains (after Moulin [15]).

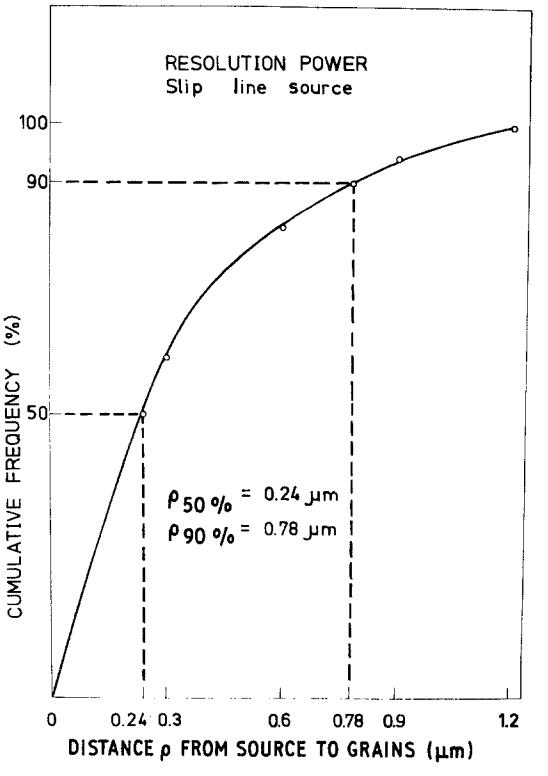

Figure 5 Location of silver grains. Cumulative frequency as a function of their distance ϱ to a linear hydrogen source (e.g. a slip line).

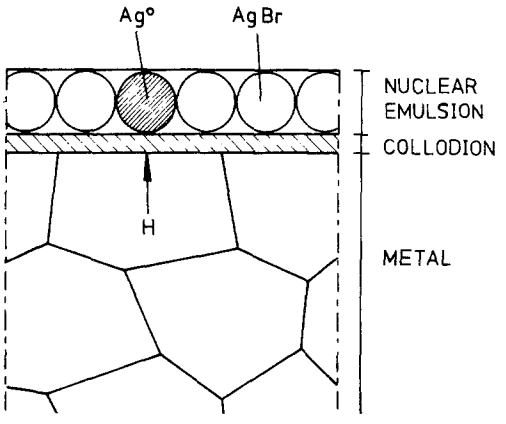

Figure 6 HMT on a surface previously coated with collodion.

plotted as the ordinate, against distances ϱ as the abscissa (Fig. 5). The power of resolution was selected as the distance for which the cumulative frequency is 50%; it corresponds to $\varrho = 0.24\,\mu m$ (240 nm). This experimental value of PR is about six times the theoretical estimate. This apparent inconsistency is ascribed to an effect related to hydrogen flux rate. For high flux, it is not only the first-neighbour AgBr crystals that are reduced, the resulting PR is larger.

It is believed that the experimental PR corresponds to an average flux rate. The slowest flux rates, that produce smaller silver-grain images and the best PR, reveal the existence of strong hydrogen traps.

3.3. Influence of protective coating

As mentioned in Section 2.2, the AgBr emulsion and the fixer produce a spurious corrosion in carbon and low-alloy steels. This corrosion masks the microstructure and impairs resolution, besides introducing false silver images (artifacts). Workers in the HPRA field dealt with this problem [12, 13] and found that a thin film of collodion, deposited on the surface before the nuclear emulsion, prevented or at least diminished corrosion and was almost transparent to electrons (Fig. 6). The substance is easy to apply in layers of say 50 nm thickness, and shows a remarkable adherence. It was proved that collodion film does not impair the hydrogen flux in our experiments with HMT. In fact, as shown in Figs. 7 and 8, the results are excellent in stainless steel with duplex structure (austenitic–ferritic). Although transparency to hydrogen was proved for the collodion film, it did not help to avoid spurious corrosion in low-carbon steel. In this case $NaNO_2$ was used as an inhibitor, both in the emulsion and in the fixer, as previously explained in Section 2.2.

Nonetheless, the presence of artifacts should always be investigated by checking several samples with a hydrogen charge and also blank samples without charge, using the same treatment in both cases.

4. Comparison with HPRA

The main features of each technique are included in Table I. A comparison is made between HPRA and HMT for the case of massive samples. In thin films, not studied as yet with our technique, the resolution of HPRA is about 0.15 μm.

5. Applications

5.1. Hydrogen evolution in a duplex stainless steel

An as-cast, Type 316-L steel were selected for this study. It was a duplex structure of austenite and δ-ferrite (14% of the latter). The steps for applications of HMT were followed as explained in Section 2. The conditions for hydrogen charge were as follows:

Electrolyte	1 N H_2SO_4 + 250 mg l^{-1} As_2O_3
Electrode	Platinum
Current density	$-20\,mA\,cm^{-2}$
Time	1 h
Temperature	Room temperature

TABLE I Comparison between HPRA and HMT

Characteristic	Tritium HPRA	HMT
Resolution (massive samples)	0.15 μm* [12]	0.04 μm* 0.25 μm†
Isotope charge	Tritium	Hydrogen
Application	Metallic materials in general	Metallic materials in general
Delay time before emulsion coating	20 h	None
Special handling	globe box, darkroom	None

*Theoretical.
†Experimental.

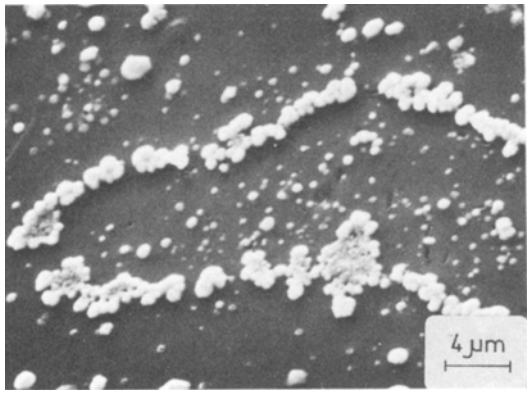

Figure 7 Duplex stainless steel. Preferential hydrogen evolution at δ–γ interface.

The time of hydrogen-evolution before emulsion coating was 2 h. The surface was protected with collodion as explained in Section 3.3. The exposure time (to hydrogen) of the emulsion was 1 h. In Figs. 7 and 8 it can be seen that hydrogen permeated through the collodion film. The results are in agreement with previous work [10], showing a preferential hydrogen desorption at the interface between austenite and δ-ferrite (Fig. 7). A distinct aggregation of silver grains is visible at the interface between matrix and inclusion (Fig. 8). The blank specimens did not show silver grains.

5.2. Hydrogen diffusivity in a cold-rolled, low-carbon steel

An AISI Type 1005, low-carbon steel was tested after 40% reduction by cold rolling. As shown elsewhere [16], this rolling generates residual tensile stress at the surface of samples less than

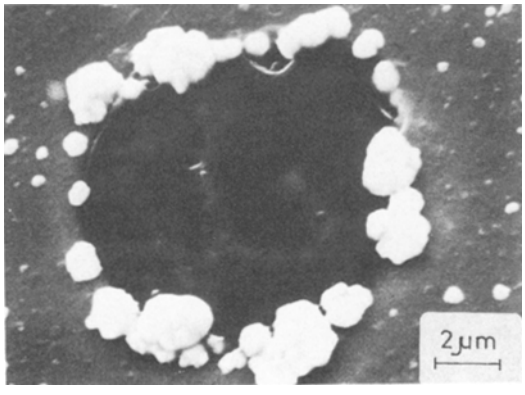

Figure 8 Duplex stainless steel. Silver grains are visible at the interface between matrix and inclusion.

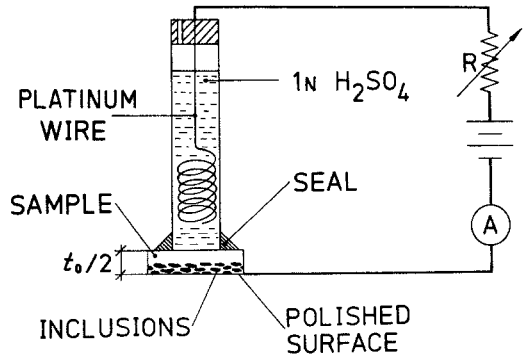

Figure 9 Experimental set-up for the hydrogen diffusivity study.

2 mm thick. In another test the rolled material was previously stress-relieved at 300° C for 1 h. The mid-section of samples was exposed by grinding one of their surfaces to 50% sample thickness ($t = t_0/2 = 0.5$ mm). The new surface was polished with 0.25 μm diamond paste, and then etched with 2% nital to reveal its microstructure.

Hydrogen charging was introduced on the opposite, untreated surface (Fig. 9) under the following conditions:

Electrolyte	1 N H_2SO_4
Current density	-5 mA cm^{-2}
Time	30 min
Temperature	Room temperature

The test surface was then covered with the nuclear emulsion, to which sodium nitrite had been added to avoid spurious corrosion (Section 2.2). The exposure time was 30 min.

Hydrogen diffusivity through the samples of thickness 0.5 mm was clearly revealed (Figs. 10 and 11). Stress-relieved samples (Fig. 10) exhibit more silver grains than samples with tensile residual stresses at their surface (Fig. 11), showing that the permeation rate is larger in the first case. It is believed that these results indicate the high sensitivity of the technique.

5.3. Hydrogen evolution in austenitic stainless steel

A Type 304-L steel was studied. Its microstructure was determined by thermal treatment as follows:

(a) Annealed at 1000° C for 1 h
(b) Sensitized at 700° C for 6 h
(c) Sensitized at 700° C for 24 h

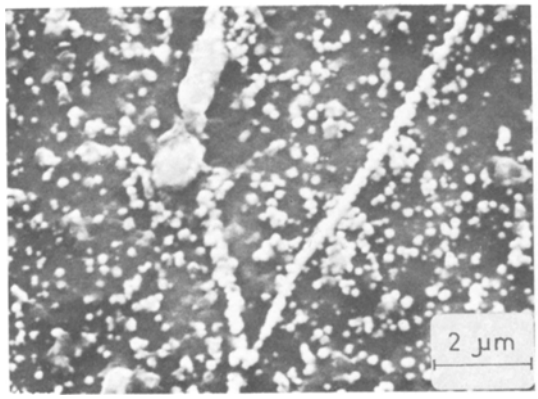

Figure 10 Hydrogen diffusivity in low-carbon steel cold-rolled and stress-relieved. Silver grains are numerous throughout and grain boundaries are clearly distinguished.

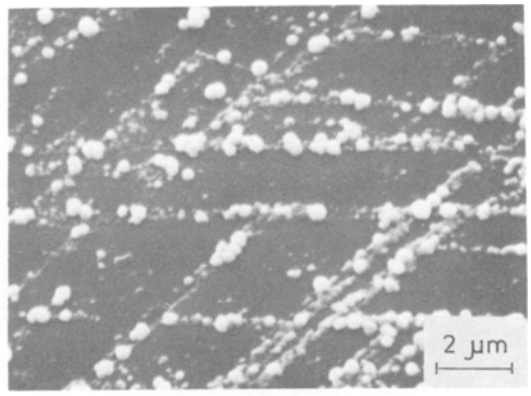

Figure 12 Austenitic stainless steel (304-L), annealed at 1000° C for 1 h. Silver grains gather at slip lines.

Treatment of the samples followed the steps described in Section 2. Hydrogen charging conditions were as specified in Section 5.1. Collodion protective coating was used in this case and hydrogen was allowed to evolve for 1 h before applying the nuclear emulsion.

It was observed that after annealing at 1000° C there is a preferential localization of silver grains at the boundaries of metallic grains, and also at twin boundaries [11]. There is also a collection of silver grains on the hydrogen-induced ε- and α′-martensites and on the deformation bands (Fig. 12).

The material sensitized at 700° C for 6 h has a discontinuous precipitation of $Cr_{23}C_6$ at grain boundaries, where a preferential localization of silver grains is observed (Fig. 13). After 24 h at 700° C, the precipitation of chromium carbide is increased. The aggregation of silver grains at sensitized grain boundaries is less than in the former case (Fig. 14). It can be inferred that the degassing rate is smaller than in the previous case, due to the interaction of hydrogen with carbides and with the hydrogen-induced ε- and α′-martensites [7]. There are also some silver grains within the austenitic grains of the sample.

6. Conclusions

1. HMT can reveal variations in the concentration of hydrogen atoms in relation to microstructural features in steels. Its sensitivity and power of resolution (Table I) enable the interpretation of hydrogen evolution from grain boundaries, twin boundaries, slip lines, hydrogen-induced ε- and α′-martensite, inclusions, microcracks and micropores.

2. The results obtained are highly reproducible.

3. Due to its characteristics, HMT should

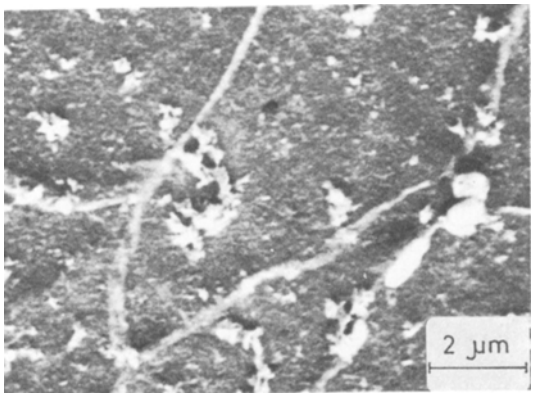

Figure 11 Hydrogen diffusivity in low-carbon steel with residual stress.

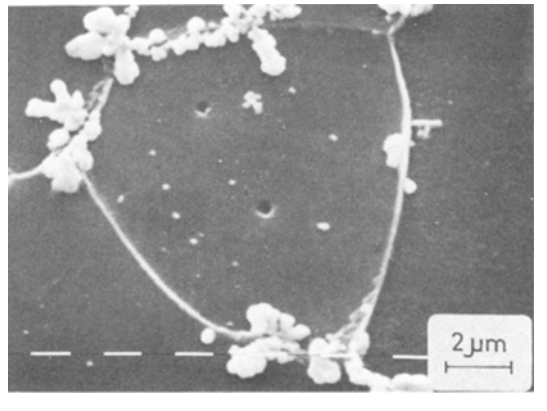

Figure 13 Austenitic stainless steel (304-L), sensitized at 700° C for 6 h. Silver grains concentrate at sensitized grain boundaries.

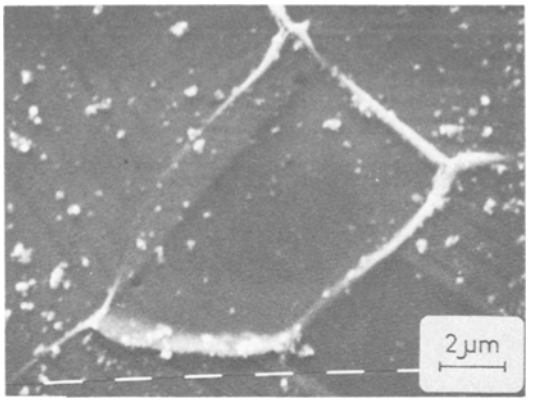

Figure 14 Austenitic stainless steel (304-L), sensitized at 700° C for 24 h. HMT shows silver grains in the matrix and at sensitized grain boundaries.

allow quantitative estimates to be made of hydrogen associated with some microstructural details.

4. Permeation studies can be followed using HMT; its rate can be determined, as well as its relationship with a specific microstructure.

5. Simplicity and precision are distinctive features of this technique, which is proving to be a valuable tool in the study of hydrogen embrittlement of metals and alloys.

Acknowledgement

I thank Dr Amílcar Funes for helpful discussions and reviewing of the manuscript.

References

1. I. M. BERSTEIN and A. W. THOMPSON, (eds) "Hydrogen in Metals" (ASM, Metals Park, Ohio, 1974).
2. P. AZOU and P. BASTIEN (eds), Proceedings of the 2nd International Congress on Hydrogen in Metals, Chatenay-Malabry, France, (Pergamon, 1977).
3. H. MATHIAS, Y. KATZ and S. NADIV, *ibid.*, paper 2C12.
4. S. TOY and A. PHILLIPS, *Corrosion* **26** (1970) 200.
5. M. AUCOUTURIER, G. LAPASSET and T. ASAOKA, *Metallurgy* **11** (1978) 5.
6. J. CHENE, J. OVEJERO-GARCÍA, C. PAES DE OLIVEIRA, M. AUCOUTURIER and P. LACOMBE, *J. Micros. Sp. Electr.* **4** (1979) 37.
7. J. OVEJERO-GARCÍA, *Metaux-Corrosion-Industrie* **674** (1981) 321.
8. T. ASAOKA, C. DAGBERT, M. AUCOUTURIER and J. GALLAND, *Scripta Metall.* **11** (1977) 467.
9. T. SCHOBER and C. DIEKER, *Metall. Trans.* **14A** (1983) 2440.
10. T. E. PÉREZ and J. OVEJERO-GARCÍA, *Scripta Metall.* **16** (1982) 161.
11. *Idem,* Proceedings of 3rd International Congress on Hydrogen and Materials, Paris, edited by P. Azou (Pergamon, 1982) p. 929.
12. J. P. LAURENT and G. LAPASSET, *Int. J. Appl. Rad. Isot.* **24** (1973) 213.
13. G. V. PRABHU-GAUNKAR, A. M. HUNTZ and P. LACOMBE, *ibid.* **30** (1979) 761.
14. T. D. LE and B. E. WILDE, Proceedings of the 1st International Conference on Current Solutions to Hydrogen Problems in Steels, Washington, 1982, edited by C. Interrante and G. Pressouyre (ASM, Metals Park, Ohio, 1983) p. 413.
15. G. MOULIN, thesis, Orsay (1981).
16. G. F. MERLONE, A. J. FUNES and J. OVEJERO-GARCÍA, to be published.

Received 30 July
and accepted 10 September 1984